An improved design for AlGaN solar-blind avalanche photodiodes with enhanced avalanche ionization*

Yin Tang(汤寅)[1], Qing Cai(蔡青)[1], Lian-Hong Yang(杨莲红)[2], Ke-Xiu Dong(董可秀)[3], Dun-Jun Chen(陈敦军)[1,†], Hai Lu(陆海)[1], Rong Zhang(张荣)[1], and You-Dou Zheng(郑有炓)[1]

[1] *Key Laboratory of Advanced Photonic and Electronic Materials, School of Electronic Science and Engineering, Nanjing University, Nanjing* 210093, *China*

[2] *Department of Physics, Changji College, Changji* 831100, *China*

[3] *School of Mechanical and Electronic Engineering, Chuzhou University, Chuzhou* 239000, *China*

(Received 11 June 2016; revised manuscript received 12 December 2016; published online 18 January 2017)

To enhance the avalanche ionization, we designed a new separate absorption and multiplication AlGaN solar-blind avalanche photodiode (APD) by using a high/low-Al-content AlGaN heterostructure as the multiplication region instead of the conventional AlGaN homogeneous layer. The calculated results show that the designed APD with $Al_{0.3}Ga_{0.7}N/Al_{0.45}Ga_{0.55}N$ heterostructure multiplication region exhibits a 60% higher gain than the conventional APD and a smaller avalanche breakdown voltage due to the use of the low-Al-content $Al_{0.3}Ga_{0.7}N$ which has about a six times higher hole ionization coefficient than the high-Al-content $Al_{0.45}Ga_{0.55}N$. Meanwhile, the designed APD still remains a good solar-blind characteristic by introducing a quarter-wave AlGaN/AlN distributed Bragg reflectors structure at the bottom of the device.

Keywords: AlGaN, deep ultraviolet, photoelectric detector, distributed Bragg reflector

PACS: 85.60.Dw, 85.60.Bt **DOI:** 10.1088/1674-1056/26/3/038503

1. Introduction

Solid-state avalanche photodiodes (APDs) based on III–nitrides have attracted increasing interest due to their excellent advantages such as lower operation voltages, lower power consumption, smaller sizes, high optical gain, high sensitivity, and no need for cooling.[1,2] AlGaN APDs with Al composition more than 40% are capable of detecting very weak ultraviolet (UV) signals in the solar-blind range ($\lambda < 290$ nm) under strong background radiation without expensive and efficiency-limiting optical filters. Such APDs could be a viable alternative to current bulky and fragile photomultiplier tubes and be widely used in many fields including missile warning and tracking, flame monitoring, ultraviolet astronomy, and bioagent detection.[3]

Great strides have been made in the realization of visible-blind GaN based APDs[4–9] and even single photon detection capabilities have been demonstrated under the Geiger mode operation.[10] However, only a few works on AlGaN solar-blind APDs have so far been reported and the multiplication gains of AlGaN solar-blind APDs reported in the literature are much lower than those of GaN APDs.[11–15] It is well-known that the causes resulted in severe degradation in performances of AlGaN solar-blind APDs and are associated with high dislocation density and low p-type doping efficiency of high-Al-content AlGaN alloys.[16,17] Another important factor is that the impact ionization coefficient decreases quickly with increasing Al content in the AlGaN alloys.[18]

In this paper, we use a high/low-Al-content AlGaN heterostructure to replace the conventional high-Al-content AlGaN homogeneous layer as the multiplication region based on a back-illuminated separate absorption and multiplication (SAM) APD in order to achieve a higher multiplication gain. The effects of the Al composition of the low-Al-content AlGaN on the gain and breakdown voltage are investigated by the simulation of the APD devices. A quarter-wave distributed Bragg reflector (DBR) structure is also introduced simultaneously to keep the solar-blind characteristic of the designed APD.

2. Structure and parameters

The schematic structure of the AlGaN solar-blind APD with an enhanced impact ionization region is shown in Fig. 1. The designed structure consists of an 800-nm-thick n-type $Al_{0.5}Ga_{0.5}N$ layer, a 180-nm-thick i-$Al_{0.45}Ga_{0.55}N$ absorption layer, a 60-nm-thick n-type $Al_{0.45}Ga_{0.55}N$ layer, an $Al_{0.3}Ga_{0.7}N$ (40 nm)/$Al_{0.45}Ga_{0.55}N$ (140 nm) heterostructure multiplication region, and a 180-nm-thick p-type $Al_{0.3}Ga_{0.7}N$ layer. It is worth noting that there exists a big potential bar-

*Project supported by the State Key Project of Research and Development Plan, China (Grant No. 2016YFB0400903), the National Natural Science Foundation of China (Grant Nos. 61634002, 61274075, and 61474060), the Key Project of Jiangsu Province, China (Grant No. BE2016174), the Anhui University Natural Science Research Project, China (Grant No. KJ2015A153), the Open Fund (KFS) of State Key Lab of Optical Technologieson Nanofabrication and Microengineering, Institute of Optics and Electronics, Chinese Academy of Science.

†Corresponding author. E-mail: djchen@nju.edu.cn

© 2017 Chinese Physical Society and IOP Publishing Ltd

rier formed in the conduction band at the heterostructure interface of the two AlGaN multiplication layers as shown in Fig. 2, which can effectively suppress the electron-initiated multiplication and would be of great benefit to reduce the APD noise. However, it can be predicted that the low-Al-content $Al_{0.3}Ga_{0.7}N$ layer may result in the loss of the solar-blind characteristic of the designed APD under high reverse bias voltages, so we introduce a quarter-wave DBR structure between the n-type $Al_{0.5}Ga_{0.5}N$ layer and the AlN template to make the APD remain a good solar-blind property. The structure of the conventional AlGaN SAM-APDs used here as a reference is similar to the designed APD except for the p-type layer, multiplication region, and the DBR structure. The 180-nm-thick p-type $Al_{0.45}Ga_{0.55}N$ layer and 180-nm-thick i-$Al_{0.45}Ga_{0.55}N$ multiplication layer are used in the conventional APD structure. For both APD structures, the hole-doping concentration for the p-type layer is 1×10^{18} cm^{-3}, while the electron-doping concentrations are 1×10^{18} cm^{-3} and 2×10^{18} cm^{-3} for the n-$Al_{0.45}Ga_{0.55}N$ and n-$Al_{0.5}Ga_{0.5}N$ layers, respectively. The residual carrier concentration for the unintentionally doped layers is 1×10^{16} cm^{-3}. The steady 2D numerical simulations are performed for the back-illuminated AlGaN SAM-APD using Silvaco Atlas software. The calculated physical model and the parameters are the same as those used in our previous work[19] except for the ionization coefficients which are extracted from Ref. [18].

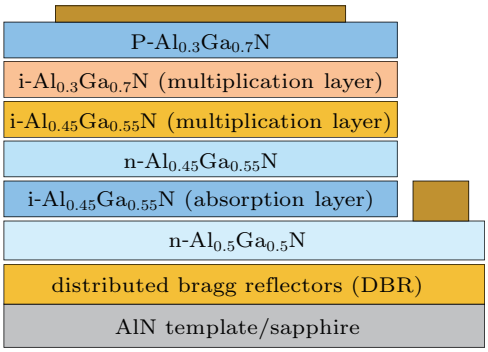


Fig. 1. (color online) Schematic structure of the designed APD.

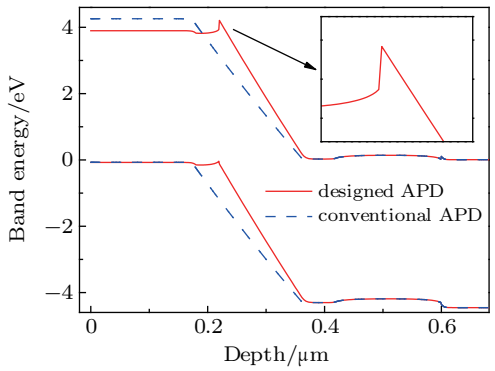


Fig. 2. (color online) The energy band diagrams of the designed and the conventional APDs under zero bias.

3. Numerical results and discussion

Figure 3 shows the current-voltage (I–V) characteristics under reverse bias in darkness and under illumination at 280 nm, and also the multiplication gains for the designed and the conventional APDs. The device size is 625 μm^2 and the power density of the incident light is 8×10^{-5} W·cm^{-2}. As observed, the dark current for the two APDs increases exponentially when the reverse bias exceeds 50 V, whilst the light current does not significantly increase until the ionization event starts at about 60 V. The avalanche gain is taken as the difference between the primary multiplied current and the multiplied dark current normalized by the difference between the primary unmultiplied current and the unmultiplied dark current.[11] The unmultiplied current is evaluated from the average value of the currents under the bias voltages between 0 and 60 V. It is indicated in Fig. 3 that the avalanche breakdown voltage shows a reduction from 113.48 V for the conventional structure to 111.05 V for the designed structure, whereas the multiplication gain increases obviously from 7.13×10^4 to 1.14×10^5 correspondingly, showing an increase of about 60%.

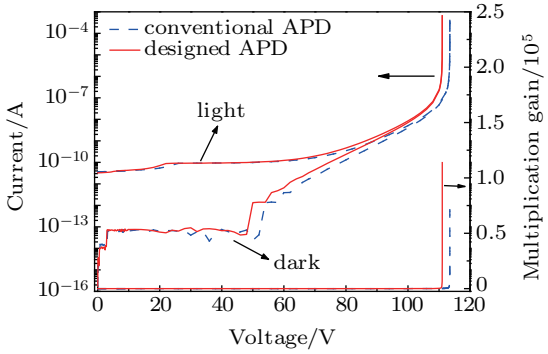


Fig. 3. (color online) I–V characteristics and multiplication gains for the conventional and the designed APDs.

To explain the discrepancies on the breakdown voltage and multiplication gain between the designed and the conventional structures, we simulate their electric field distributions at the voltage point with maximum multiplication gain as shown in Fig. 4. We can find that the electric field strength increases slightly at the high-Al-content $Al_{0.45}Ga_{0.55}N$ layer and decreases significantly at the low-Al-content $Al_{0.3}Ga_{0.7}N$ layer for the designed APD structure compared to that of the conventional structure. The required avalanche electric field decreases significantly at the low-Al-content $Al_{0.3}Ga_{0.7}N$ layer as expected thanks to the reduced band gap, which is beneficial to obtain a higher gain. Further, the hole impact ionization coefficient increases remarkably with decreasing Al composition in the AlGaN alloys according to Ref. [18], about six times higher using the low-Al-content $Al_{0.3}Ga_{0.7}N$ instead of the high-Al-content $Al_{0.45}Ga_{0.55}N$ layer. So the designed APD structure can obtain a remarkably higher gain than the conventional APD structure.

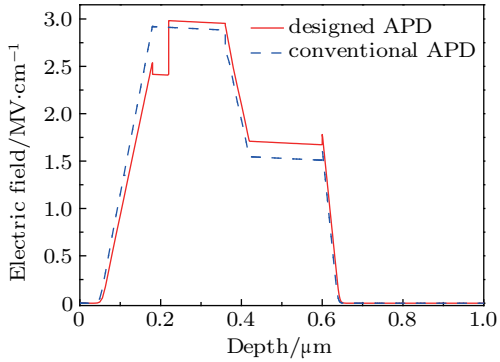


Fig. 4. (color online) The electric field distributions of the conventional and the designed APDs at the voltage point with maximum multiplication gain.

We calculate the multiplication gain and the avalanche breakdown voltage of the designed structure with different low-Al-content AlGaN layers, as shown in Fig. 5. In addition, the Al composition of the p-type AlGaN layer is kept consistent with the low-Al-content AlGaN layer. When the Al composition of the low-Al-content AlGaN layer decreases, thanks to the higher hole impact ionization coefficient, the designed APD exhibits an increasing multiplication gain and a decreasing avalanche breakdown voltage. It means that we can obtain a higher multiplication gain and a lower avalanche breakdown voltage by using a lower Al-content AlGaN layer. However, the use of the low-Al-content AlGaN layer in the multiplication region can result in the loss of the solar-blind characteristic of the APDs. In order to retain the solar-blind characteristic of the designed APDs, we introduce a quarter-wave distributed Bragg reflector (DBR) structure between the n-type $Al_{0.5}Ga_{0.5}N$ layer and the AlN template. The DBR materials chosen here are $Al_xGa_{1-x}N$/AlN bilayer thin films, which have been investigated extensively.[20,21] The Al composition x in $Al_xGa_{1-x}N$/AlN DBR should be larger than 0.4 at least in order to guarantee the transmission of light in the solar-blind range. According to the $Al_xGa_{1-x}N$/AlN DBR properties and the request of solar blind, we design a 27.5 pairs $Al_{0.5}Ga_{0.5}N$/AlN periodic structure with a central wavelength of 300 nm. The thicknesses of the AlN and $Al_{0.5}Ga_{0.5}N$ layers are 34.25 nm and 30.85 nm decided by the formula $d_{\mathrm{AlN}} = \lambda/4n_{\mathrm{AlN}}$ and $d_{\mathrm{AlGaN}} = \lambda/4n_{\mathrm{AlGaN}}$. Here $n_{\mathrm{AlN}}(= 2.190)$ and $n_{\mathrm{AlGaN}}(= 2.431)$ are the refractive coefficients of AlN and $Al_{0.5}Ga_{0.5}N$, which are extracted from Ref. [22]. Figure 6 shows the calculated reflectivity spectrum of the DBR structure by the transfer matrix method. It can be seen that the DBR maintains a high reflectance of 95%–99.9% in the wavelength range of 290–310 nm, where the long wavelength side of the high reflectance region just corresponds to the band gap energy of the $Al_{0.3}Ga_{0.7}N$ alloy. Therefore, taking into account the gain and solar-blind characteristic, the Al composition of 30% in the low-Al-content AlGaN layer will be a compromising choice, which can obtain a high gain and keep a good solar-blind characteristic simultaneously.

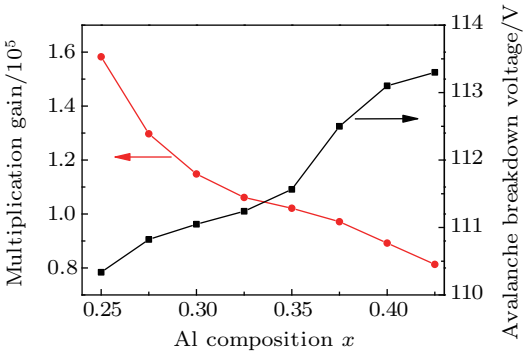


Fig. 5. (color online) The calculated multiplication gain and the avalanche breakdown voltage of the designed structure with different low-Al-content AlGaN layers.

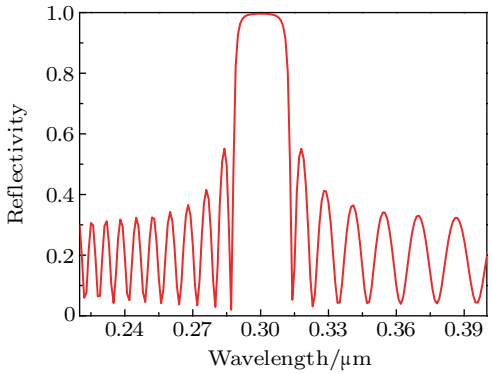


Fig. 6. (color online) Reflectivity spectrum of the DBR structure.

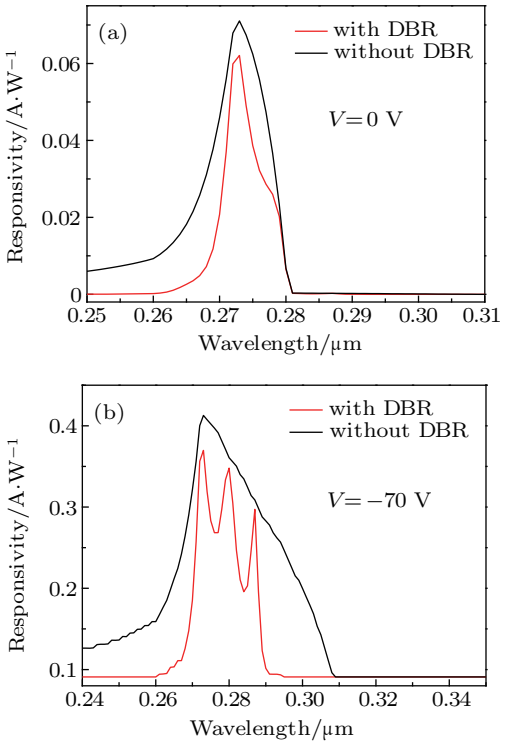


Fig. 7. (color online) Spectral responsivities of the designed APDs with $Al_{0.3}Ga_{0.7}N$ /$Al_{0.45}Ga_{0.55}N$ heterostructure multiplication region in both cases with and without the DBR structure at 0 V and −70 V.

Figure 7 shows the spectral responsivities of the designed APDs with $Al_{0.3}Ga_{0.7}N$ /$Al_{0.45}Ga_{0.55}N$ heterostructure multiplication region under back illumination in both cases with

and without the DBR structure. As shown in Fig. 7(a), the designed APDs with and without the DBR structure both present a sharp cutoff at 280 nm at zero bias, and the photocurrent response from the low-Al-content $Al_{0.3}Ga_{0.7}N$ layer is not observed in the case even without the DBR structure, indicating that the barrier formed in the conduction band at the $Al_{0.3}Ga_{0.7}N/Al_{0.45}Ga_{0.55}N$ heterostructure interface effectively suppresses photocurrent generated in the low-Al-content $Al_{0.3}Ga_{0.7}N$ layer. When the reverse bias reaches 70 V where the ionization event has started, the spectral responsivity of the designed APD with the DBR structure, as shown in Fig. 7(b), presents a sharp cutoff at 290 nm, which remains the solar-blind characteristic. However, for the APD without the DBR structure, the cutoff wavelength of the spectral responsivity shifts to 308 nm as expected, corresponding to the absorption edge of $Al_{0.3}Ga_{0.7}N$.

4. Conclusion

In summary, an enhanced avalanche ionization region was designed based on a separate absorption and multiplication AlGaN solar-blind APD structure. The designed APD with an $Al_{0.3}Ga_{0.7}N/Al_{0.45}Ga_{0.55}N$ heterostructure as the multiplication region instead of the conventional AlGaN homogeneous layer exhibits about a 60% higher multiplication gain and a lower avalanche breakdown voltage in comparison to the conventional APD. Meanwhile, the designed APD can still retain a good solar-blind characteristic by introducing a proper DBR structure at the bottom of the device.

References

[1] Pau J L, Bayram C, McClintock R, Razeghi M and Silversmith D 2008 *Appl. Phys. Lett.* **92** 101120

[2] Wang X D, Hu W D, Pan M, Hou L W, Xie W, Xu J T, Li X Y, Chen X S and Lu W 2014 *J. Appl. Phys.* **115** 013103

[3] Bulmer J, Suvarna P, Leathersich J, Marini J, Mahaboob I, Newman N and Shadi F 2016 *IEEE Photon. Technol. Lett.* **28** 1

[4] McIntosh K A, Molnar R J, Mahoney L J, Lightfoot A, Geis M W, Molvar K M, MeIngailis I, Aggarwal R L, Goodhue W D, Choi S S, Spears D L and Verghese S 1999 *Appl. Phys. Lett.* **75** 3485

[5] Carrano J C, Lambert D J H, Eiting C J, Collins C J, Li T, Wang S, Yang B, Beck A L, Dupuis R D and Campbell J C 2000 *Appl. Phys. Lett.* **76** 924

[6] Limb J B, Yoo D, Ryou J H, Lee W, Shen S C, Dupuis R D, Reed M L, Collins C J, Wraback M, Hanser M, Preble E, Williams N M and Evans K 2006 *Appl. Phys. Lett.* **89** 011112

[7] Vashaei Z, Cicek E, Bayram C, McClintock R and Razeghi M 2010 *Appl. Phys. Lett.* **96** 201908

[8] Bayram C, Pau J L, McClintock R, Razeghi M, Ulmer M P and Silversmith D 2008 *Appl. Phys. Lett.* **93** 211107

[9] Kim J, Ji M H, Detchprohm T, Dupuis R D, Ryou J H, Sood A K, Dhar N D and Lewis J 2015 *Appl. Phys. Express* **8** 122202

[10] Pau J L, McClintock R, Minder K, Bayram C, Kung P, Razeghi M, Munoz E and Silversmith D 2007 *Appl. Phys. Lett.* **91** 041104

[11] Mcclintock R, Yasan A, Minder K, Kung P and Razeghi M 2005 *Appl. Phys. Lett.* **87** 241123

[12] Tut T, Gokkavas M, Inal A and Ozbay E 2007 *Appl. Phys. Lett.* **90** 163506

[13] Huang Y, Chen D J, Lu H, Dong K X, Zhang R, Zheng Y D, Li L and Li Z H 2012 *Appl. Phys. Lett.* **101** 253516

[14] Huang Z Q, Li J F, Zhang W L and Jiang H 2013 *Appl. Phys. Express* **6** 054101

[15] Shao Z G, Chen D J, Lu H, Zhang R, Cao D P, Luo W J, Zheng Y D, Li L and Li Z H 2014 *IEEE Electron Device Lett.* **35** 372

[16] Sun L, Chen J L, Li J F and Jiang H 2010 *Appl. Phys. Lett.* **97** 191103

[17] Yang B, Li T, Heng K, Collins C, Wang S, Carrano J C, Dpuis R D, Campbell J C, Schurman M J and Ferguson I T 2000 *IEEE J. Quantum Electron* **36** 1229

[18] Bellotti E, Bertazzi F, Shishehchi S, Matsubara M and Goano M 2013 *IEEE Trans. Electron Devices* **60** 3204

[19] Dong K X, Chen D J, Lu H, Liu B, Han P, Zhang R and Zheng Y D 2013 *IEEE Photon. Technol. Lett.* **25** 1510

[20] Mitrofanov O, Schmult S, Manfra M J, Siegrist T, Weimann N G, Sergent A M and Molnar R J 2006 *Appl. Phys. Lett.* **88** 171101

[21] Ji X L, Jiang R L, Liu B, Xie Z L, Zhou J J, Li L, Han P, Zhang R, Zheng Y D and Zheng J G 2008 *Phys. Stat. Sol. (A)* **205** 1572

[22] Brunner D, Angerer H, Bustarret E, Freudenberg F, Hopler R, Dimitrov R, Ambacher O and Stutzmann M 1997 *J. Appl. Phys.* **82** 5090